

Introduction of titanium species into fluorine-modified SiO₂- supported Cr-V bimetallic catalyst for ethylene polymerization and ethylene/1-hexene copolymerization

Qiaqiao Sun, Ruihua Cheng*, Zhen Liu, Xuelian He, Ning Zhao, Boping Liu*

State Key Lab of Chemical Engineering, East China University of Science and Technology, Meilong Road 130, Shanghai 200237, P. R. China

Received: 22 January 2017 Accepted: 13 May 2017

ABSTRACT

Chromium-vanadium (Cr-V) bimetallic catalysts are prepared by the introduction of vanadium into the Phillips catalyst which is one of the most significant industrial ethylene polymerization catalysts for tuning the Phillips catalyst performances and improving polyethylene properties. In the present work, titanium species were introduced into the fluorine-modified chromium-vanadium bimetallic catalysts (Cr-V-F) and the prepared catalysts were systematically explored. The element content results of multi-component catalysts showed that a competitive inhibition interaction existed between chromium and vanadium, whereas chromium was more preferable to attach to the Ti-SiO₂ than vanadium. In addition, ethylene homopolymerization and ethylene/1-hexene copolymerization were carried out and examined with different catalysts. The introduction of titanium into fluorine-modified bimetallic catalysts enhanced the molecular weight (MW) and broadened the molecular weight distribution (MWD) of polyethylene. The MW of the titanium- and fluorine-modified bimetallic catalysts (Cr-V-F/Ti) firstly rose up and then dropped down with the increasing of the Al/Cr molar ratio. The Cr-V-F/Ti catalysts showed slightly depressed hydrogen response and incorporation of 1-hexene. The short-chain branch distribution (SCBD) results, which were characterized by TREF/SSA, showed that the introduction of the titanium species increased the SCB content in low MW fractions and decreased the SCB content in the high M_w fractions of ethylene/1-hexene copolymers obtained from (Cr-V-F/3Ti)⁶⁰⁰ in contrast to that from (Cr-V-F)⁶⁰⁰. **Polyolefins J (2017) 4: 221-234**

Keywords: Ethylene polymerization; bimetallic catalyst; titanium modification; fluorine modification; short-chain branch distribution.

INTRODUCTION

As the most commonly used plastic in the world, polyethylene (PE) is used for the fabrication of blow-molded containers, extruded pipes, sheeting and packing materials, etc. Different forms of PE can be produced by transition metal-catalyzed olefin polymerization. The inorganic chromium-based catalyst, namely, Phillips catalyst invented by Hogan and Banks is one of the most important industrial catalysts accounts for

more than 40 % of high density polyethylene (HDPE) [1-4]. The traditional Phillips catalyst is prepared by the impregnation of an aqueous solution of a chromium compound with a high-surface-area carrier such as silica and then activated by calcination in dry air or oxygen at an elevated temperature, generally 500-1000°C [1-6].

During the past decades, a variety of chemical modifications have been carried out to tune the Phillips catalyst performance, such as chemical modification of the support [5, 7-17], and the introduction of other

* Corresponding Author - E-mail: rhcheng@ecust.edu.cn, boping@ecust.edu.cn

transition metals to prepare bimetallic or multi-metallic Phillips catalyst [18-22]. Practically speaking, organic chromium or many other metal oxides are introduced to Phillips catalyst as modifiers [18-22]. To tune the catalyst performances and the obtained polymer properties, bis(triphenylsilyl) chromate was introduced to traditional Phillips catalyst by using the residual surface hydroxyl groups in Phillips catalyst support [19]. Vanadium, which is situated between chromium and titanium in the periodic system, is not only the active component of classic vanadium–magnesium catalysts but also it is the active component of other vanadium-based catalyst systems for ethylene polymerization [27-36]. Vanadium is introduced to Phillips catalyst for the sake of α -olefin incorporation enhancement and molecular weight (MW) regulation. A series of vanadium-modified Phillips catalysts were prepared by Akanksha Matta et al. [21] through co-impregnation procedures in order to improve the branching ability of Phillips catalyst for ethylene polymerization. Also his work showed that the performance of vanadium-modified Phillips catalyst was influenced by the kind of vanadium precursors, the pH of impregnation solution and the vanadium fluoride-containing compound powers. The activity of the catalyst, activated at low temperature, is improved by fluorine modification and the resulting high molecular weight polyethylene can be used for manufacturing of large containers, especially fuel tanks. However, the catalyst supports are easily to sinter at a higher activation temperature due to the addition of fluorine. A series of patents and papers [5, 7-12, 15] have reported that titanium-modified silica, which is applied as a support for Phillips catalyst, promotes the catalyst activity and lowers the polymer molecular weight due to the fact that the addition of titanium improves the Brønsted acidity of the silica surface. Two common techniques for the preparation of Cr/silica-titanium catalyst, which are commercially used, are impregnating the silica with a titanium compound followed by calcinations, and preparing a silica-titania “cogel” through dissolving a titanium salt and adding silica. Our group [20] developed a SiO₂-supported inorganic chromium oxide/inorganic vanadium oxide bimetallic catalyst which showed high activity and 1-hexene incorporation into higher molecular weight fraction too. The SiO₂-supported chromium oxide/vanadium oxide bimetallic catalyst was prepared with the introduction of vanadium oxide into the traditional

Phillips catalyst and the polymerization activity was significantly enhanced compared with the activity of the polymerization by the Phillips catalyst. The short-chain branch distribution of the obtained bimodal ethylene/1-hexene copolymer was improved by the novel bimetallic catalyst, but only with more 1-hexene comonomer insertion into the high MW part without the reduction of 1-hexene comonomer insertion into the low MW part. Halide groups are introduced onto the surface of silica support to replace surface silanol groups of the Phillips catalyst and fluoride is the most easily utilized [4, 8, 12-14, 23, 24]. The fluorine can be added to the Phillips catalyst by impregnation with a fluoride-containing aqueous solution or by dry mixing with fluoride-containing compounds as powders. Many patents and papers [4, 14, 23, 25] published on novel fluorine-modified Phillips catalysts showed that the supports containing titanium were preferable for fluorine modification. On the one hand, fluorine-modified Cr/silica–titania catalyst was less sensitive to the fluoride-catalyzed sintering. In addition, the presence of fluorine on a Cr/silica–titania catalyst promoted the incorporation efficiency of α -olefins such as 1-hexene.

In the present work, we introduced titanium species into the fluorine-modified chromium-vanadium bimetallic (Cr-V-F) catalysts to prepare a series of titanium- and fluorine-modified Cr-V bimetallic catalysts (Cr-V-F/Ti) to explore the effects of the introduction of titanium to fluorine-modified Cr-V bimetallic catalysts on the polymerization behavior and catalyst activity. The properties of different catalysts were characterized. Additionally, ethylene homopolymerization and ethylene/1-hexene copolymerization were conducted and examined with different catalysts. The SCBD of copolymer was characterized through HT-GPC, DSC and TREF/SSA methods.

EXPERIMENTAL

Raw materials

In this work, chromium (III) acetate hydroxide (with 24 wt% Cr, AR grade) was purchased from Johnson Matthey Company. Ammonium metavanadate and tetra-n-butyl titanate (TBT) were purchased from Sinopharm Chemical Reagent Co., Ltd. Ammonium fluorosilicate was purchased from Aladdin Company.

Triisobutylaluminium (TIBA, 1.0 M in heptane) was purchased from Alfa Aesar. Silica gel (Davison 955) was donated by Qilu Branch Co., SINOPEC. Pure dry air (> 99.999 %) and high purity hydrogen (> 99.999 %) were supplied by Shanghai Wetry Criterion Gas. Co., Ltd. The high purity N₂ (> 99.999 %) used in the catalyst preparation process and the ethylene used in the polymerization reactions were purified by passing through columns of 4A molecular sieves and silver molecular sieves for dehydration and deoxidation, respectively. n-Hexane (AR grade) and n-heptane (AR grade) were purchased from Sinopharm Chemical Reagent Co., Ltd and purified by distillation in the presence of sodium metal slices with diphenyl ketone as indicator ahead of application. 1-Hexene (total purity 97 %) as comonomer was purchased from J&K Chemical Co., and purified in the same way as n-hexane (AR grade) and n-heptane (AR grade) and then transferred into a storage tank under purified nitrogen atmosphere after diphenyl ketone showed pure blue.

Catalyst preparation

A series of Cr-V-F/Ti catalysts and Cr-V-F catalysts as references were prepared. The chromium loading was 1.0 wt% and the Cr/V molar ratio was 2:1[20]. The Cr-V-F catalysts were prepared through a co-impregnation procedure by impregnation of 10 g silica gel (dried at 120°C for 6 h) with the mixed aqueous solutions of certain amount of chromium (III) acetate hydroxide, ammonium metavanadate, and ammonium fluorosilicate at 50°C for 4 h and followed by being dried at 120°C for 12 h. Then, the obtained sample was transferred into a fluidized-bed reactor in order to calcine at a target temperature under high purity dry air atmosphere with a flow rate of 600 mL/min for 6 h after calcination at 150°C in dried N₂ flow for 1.5 h. Finally, the catalyst sample was cooled down under dried N₂

and stored in glass ampoule bottles in a glove box.

The Cr-V-F/Ti catalysts preparation procedures consist of two parts: Firstly, the titanium-modified silica was prepared by treating 10 g virgin silica gel (dried at 120°C for 6 h) with a certain amount of TBT in n-hexane at ambient temperature for 4 h and drying at 80°C at atmospheric pressure for 4 h and in vacuum for 4 h. Subsequently, the dried sample was calcinated at 600°C in dry air for 4 h in a fluidized-bed quartz reactor. The obtained titanium-modified silica was cooled down to room temperature in N₂ and transferred into a storage jar for the next step. In the second step, the titanium-modified silica was impregnated with the mixed aqueous solutions of certain amount of chromium (III) acetate hydroxide, ammonium metavanadate, and ammonium fluorosilicate at 50°C for 4 h and dried at 120°C for 12 h. Then, the obtained sample was transferred into a fluidized bed to calcine at a target temperature under high purity dry air atmosphere with a flow rate of 600 mL/min for 6 h after calcination at 150°C in dried N₂ flow for 1.5 h. Finally, the catalyst sample was cooled down under dried N₂ atmosphere and then stored in glass ampoule bottles in a glove box. The detailed information of the catalysts is listed in Table 1.

Characterization of catalysts

Inductively coupled plasma (ICP)

The chromium, vanadium, and titanium contents in the prepared catalysts were identified by ICP characterization. The power of the ICP spectrometer (Varian 710-ES) was 1.10 kW. The flow rates of plasma gas and auxiliary gas were 15.0 and 1.50 L/min, respectively. The pressure of nebulizing gas was 200 kPa and the pump speed was 13 rpm.

Nitrogen adsorption/desorption experiments

The physical adsorption/desorption measurements

Table 1. Preparation methods and compositions of the catalysts studied.

Catalyst Sample	Impregnation methods	Activation temperature [°C]	Cr wt%	V wt%	F wt%	Ti wt%
(Cr-V-F) ⁶⁰⁰	Co-impregnation	600	1.0	0.48	1.5	0
(Cr-V-F) ⁵⁰⁰	Co-impregnation	500	1.0	0.48	1.5	0
(Cr-V-F/3Ti) ⁶⁰⁰	Two-step impregnation ^(a)	600	1.0	0.48	1.5	3.0
(Cr-V-F/3Ti) ⁵⁰⁰	Two-step impregnation ^(a)	500	1.0	0.48	1.5	3.0
(Cr-V-F/6Ti) ⁵⁰⁰	Two-step impregnation ^(b)	500	1.0	0.48	1.5	6.0

^(a) Two-step impregnation procedure, Ti was first loaded on the silica, dried and calcined at 600 °C, then the Cr, V and F were loaded; the Ti-loading was 3.0 wt%.

^(b) Two-step impregnation procedure, Ti was first loaded on the silica, dried and calcined at 600 °C, then the Cr, V and F were loaded; the Ti-loading was 6.0 wt%.

of N₂ were carried out on a Micrometrics ASAP 2020 V3.00 H system at -196°C after degassing each sample (0.1 g) under vacuum at 400°C for 1 h in order to obtain the specific surface area, pore volume and average pore size of the silica gel and catalysts.

Scanning electron microscope (SEM)

The SEM observation of surface structure of the silica gel and catalysts was performed on NOVA Nano SEM450. The resolution in high vacuum mode at the low voltage of 1kV was 1.4 nm and the highest resolution of 1.8 nm was obtained at low voltage of 3 kV. The accelerating voltage was 200 V – 30 kV. The current density was 0.6 pA – 200 nA.

Ethylene, ethylene/1-hexene polymerization

Ethylene and ethylene/1-hexene polymerization of different catalysts were operated in a semi-batch slurry polymerization run. The reactions were carried out in a 250 mL three-necked flask reactor with continuous purified ethylene at 0.15 MPa at certain temperatures for 1 h. The dilute TIBA as cocatalyst was added after the addition of 70 mL n-heptane as solvent to the reactor with a certain stirred rate. The ethylene consumption rate was collected by an automatic data acquisition system (Brooks Instrument 0150E) to investigate the reaction kinetics. The polymerization was terminated by adding 100 mL ethanol/HCl solution. After washing with ethanol, the products were dried at 60°C under vacuum for 6 h and the weight would be corresponded to the catalyst polymerization activity.

The H₂ response or ethylene/1-hexene copolymerization experiments were performed through injecting certain amount of H₂ or 1-hexene as comonomer into the flask, and adding the cocatalyst. Other operations were as the same as the ethylene homopolymerization as stated above.

Polymer characterizations

High temperature gel permeation chromatography (HT-GPC)

The MW and MWD of the polymers were measured by an Agilent PL-220 high temperature gel permeation chromatograph (HT-GPC) with two PL gel-Olexis columns at a flow rate of 1 mL/min at 160°C using 1,2,4-trichlorobenzene (TCB) as solvent and polystyrene (PS) as standard sample, respectively. Dissolution of the polymers in stabilized TCB was carried out by heating at 160°C for 5 h under

continuous gentle agitation.

Differential scanning calorimetry (DSC)

Melting temperature (T_m) and crystallinity (%) were measured by differential scanning calorimetry (DSC) experiments on a TA Q200 DSC machine. About 5mg polymer sample was weighted and then heated to 150°C at 10°C /min and kept for 5 min to remove thermal history and then cooled down to 40°C at 10°C /min, and finally up to 150°C at 10°C /min under N₂ atmosphere. The melting temperature (T_m) and crystallinity (%) of each sample were calculated using the DSC curves.

High-Temperature ¹³C NMR (HT-¹³C NMR)

The 1-hexene incorporation was measured by high-temperature ¹³C NMR (HT-¹³C NMR); each sample (100 mg) was equipped with a 5 mm NMR tube using 1,4-dichlorobenzene-d₄ (DCB-d₄) as solvent (sample concentration ~15 mg/mL) and scanned by Varian Mercury Plus 300 at 130°C, at 100.62 MHz with delay index of 3 s for 10 h. The carbon in the polymer chain backbone was regarded as the internal reference at 30.00 ppm. The inserted 1-hexene content of each sample was calculated according to normalized integrating area in the ¹³C NMR spectrum according to the Seger's work for reference [26].

Temperature rising elution fractionation (TREF)

The ethylene/1-hexene copolymers were fractionated by a self-made TREF system [19, 20, 27, 28], which included an 850 mL column type fractionation bottle filled with quartz sand, a silicone oil bath with thermostat (Huber, POLYTSTAT CC2-225B ± 0.02°C), a pump (KNF Lab, STEPDOS 08 S), and a rotary evaporator (EYELA). The process was performed under N₂ atmosphere.

Approximately 1.2 g copolymer sample was dissolved in 200 mL xylene in a three-necked flask by stirring for 2.5-3 h and the solution was rapidly transferred into the preheated fractionation bottle. The sample solution was kept at 135°C for 1 h and then cooled down to 40°C at 5°C/h. After the cooling step, the temperature was raised up to the selected elution temperature and kept for 1 h for dissolution of the corresponding fraction step-by-step. The solvent of each fraction was removed by rotary evaporator, and each fraction was deposited with isopropyl alcohol and finally vacuum dried at 60°C for 12 h. More details

Table 2. Composition of the catalyst samples.

	Activation temperature [°C]	Cr [wt%]	Cr ^(a) [wt%]	V [wt%]	V ^(a) [wt%]	Ti [wt%]	Ti ^(a) [wt%]
(Cr-V-F) ⁶⁰⁰	600	1.0	0.72	0.48	0.44	-	-
(Cr-V-F) ⁵⁰⁰	500	1.0	0.81	0.48	0.42	-	-
(Cr-V-F/3Ti) ⁶⁰⁰	600	1.0	0.75	0.48	0.47	3.0	1.3
(Cr-V-F/3Ti) ⁵⁰⁰	500	1.0	0.79	0.48	0.46	3.0	1.3
(Cr-V-F/6Ti) ⁵⁰⁰	500	1.0	0.89	0.48	0.38	6.0	2.8

^(a) Measured by ICP.

could be found in our previous work [19, 20, 28].

Successive self-nucleation and annealing (SSA)

The SSA curves of obtained copolymer fractions were recorded by a TA Q200 DSC machine under N₂ atmosphere, and according to a general research approach [29-31] were used to characterize the lamella thickness distribution of the polymers. The detailed temperature program was referenced in our previous work [19, 20, 28].

RESULTS AND DISCUSSION

Characterization of catalysts

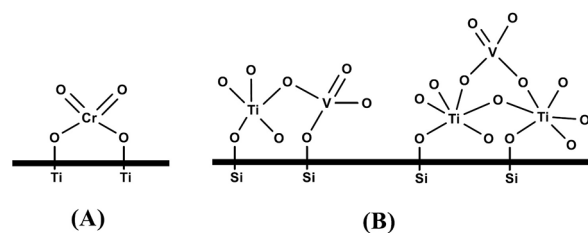
The element contents of catalysts were characterized by ICP and the results are shown in Table 2. First, it was notable that the actual Ti loading was just nearly half of the initial addition value, which was probably due to the mass loss in the impregnation step and the calcination step. Second, the total actual Cr and V loadings remained relatively stable without significant loss. The actual V loading of (Cr-V-F/3Ti)⁶⁰⁰ and (Cr-V-F/3Ti)⁵⁰⁰ in the case of 3 wt% (theoretical loading value) Ti loading was more than that of untitanated (Cr-V-F)⁵⁰⁰, but the value declined when 6 wt% (theoretical loading value) Ti was added. Reversely, the actual Cr loading of (Cr-V-F/6Ti)⁵⁰⁰ was more than low-titanium-content catalysts and (Cr-V-F)⁵⁰⁰. Pullukat and Shida [32] and Pullukat et al. [33] using X-ray photoelectron spectroscopy, optical spectroscopy, and polymerization kinetics illustrated that the Cr (VI) was attached onto the titanium surface through oxygen atom, as shown in Scheme 1 (A). The molecular structures of the surface vanadium oxide species on Ti-SiO₂, shown in Scheme 1 (B) could be concluded by in-situ Raman, UV-vis-NIR diffuse reflectance, X-ray absorption near-edge, and X-ray photoelectron spectroscopies by

Gao and his coworkers [34, 35]. In the present study, the element contents resulted from multi-component catalysts showed a competitive inhibition interaction between chromium and vanadium. Overall, the actual chromium loading and vanadium loading as the effective active components of catalysts were not far off the theoretical values.

The porosity of support affects the microstructures and properties of the polyethylene product [36-39]. The results of the nitrogen adsorption/desorption experiments, which were applied to determine the surface area and pore structure parameters, are listed in Table 3. The surface area, pore volume, and pore size of the catalysts decreased in comparison to those of virgin silica gel, which could owe to the catalytic components supported on the surface of SiO₂ support. With the addition of titanium, the pore size of the catalyst became larger than the pore size of (Cr-V-F)⁵⁰⁰. The surface area, pore volume, and average pore size of each catalyst remained at a good level. The images of SEM in Figure S1 showed that the virgin silica gel particles were almost spherical and had a smooth surface. Compared with the virgin silica gel, the catalysts were broken into fragments of different sizes by the stirring magnetic bar during catalyst preparation.

Homopolymerization behavior of different bimetallic catalysts

Ethylene homopolymerization reactions of the



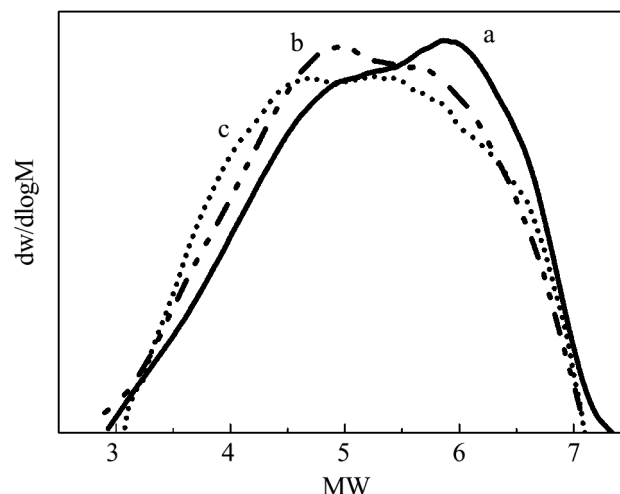
Scheme 1. Molecular structures of the surface oxides species on silica supposed in lectures: (A) Molecular structures of the surface titanium oxide species on Ti-SiO₂, (B) Molecular structures of the surface vanadium oxide species on Ti-SiO₂.

Table 3. Physical properties of the calcinated support and catalyst samples^(a).

	Specific surface area [m ² /g]	Pore volume [cm ³ /g]	Average pore size [nm]
SiO ₂	280.9	1.66	23.70
(Cr-V-F) ⁵⁰⁰	247.0	1.36	21.45
(Cr-V-F/3Ti) ⁶⁰⁰	230.0	1.33	23.04
(Cr-V-F/3Ti) ⁵⁰⁰	225.3	1.29	22.11

^(a)Measured by nitrogen adsorption/desorption experiments.

modified Cr-V bimetallic catalysts were performed at 85°C and at 0.15 MPa in heptane as solvent with TIBA acted as cocatalyst. The ethylene homopolymerization reaction activities and the properties of the polymers are listed in Table 4. The activities of (Cr-V-F/3Ti)⁵⁰⁰ and (Cr-V-F/6Ti)⁵⁰⁰ were slightly increased by the addition of titanium in comparison with that of (Cr-V-F)⁵⁰⁰. According to the literature report of the study of titanium-modified Phillips catalyst [5, 7-11], the overall activity was increased by the addition of a few percent of titanium. Similarly, the activity of (Cr-V-F/6Ti)⁵⁰⁰ with 6 wt% Ti loading was lower than that of (Cr-V-F/3Ti)⁵⁰⁰ with 3 wt% Ti loading. The activity of (Cr-V-F/3Ti)⁵⁰⁰ activated at 500°C was higher than that of (Cr-V-F/3Ti)⁶⁰⁰ activated at 600°C of which Ti loading was both the same. The MWD of the polyethylene obtained from the (Cr-V-F/3Ti)⁶⁰⁰, (Cr-V-F/3Ti)⁵⁰⁰, and (Cr-V-F/6Ti)⁵⁰⁰ catalyzed polymerization were all above 39.0 while the MWD of the polyethylene obtained from the (Cr-V-F)⁶⁰⁰ and (Cr-V-F)⁵⁰⁰ catalyzed polymerization were both below 28.0 as listed in Table 4. The introduction of titanium into the F-modified bimetallic catalysts brought the increase of MW and broadened the MWD of polyethylene as depicted in Figure 1. After titanium modification, the lower molecular weight part of polyethylene increased. The narrower MWD of (Cr-V-F/6Ti)⁵⁰⁰ as against that of (Cr-V-F/3Ti)⁵⁰⁰ indicated that the active species of (Cr-V-F/6Ti)⁵⁰⁰ were more uniform, which might attribute to the high Ti loading. Both the activity and MW of (Cr-V-F/3Ti)⁵⁰⁰ were the

**Figure 1.** GPC curves of ethylene homopolymerization different catalysts: (a) (Cr-V-F)⁵⁰⁰, (b) (Cr-V-F/3Ti)⁵⁰⁰, and (c) (Cr-V-F/6Ti)⁵⁰⁰.

highest among the four catalysts.

Though Phillips catalyst does not require cocatalyst, the addition of small amounts of cocatalyst to the reactor can improve the polymerization activity and modify the obtained polyethylene [40-45]. TIBA is one of the commonly used cocatalysts in industrial applications. A small amount of TIBA can serve as scavengers, removing trace levels of poisons such as oxygen and water as well as removing redox by-products in induction period [4, 46]. Unfortunately, too much of TIBA can lead to a loss of polymerization activity by over-reduction of active species or attacking the Cr-support bonds in the study of Phillips catalyst. The ethylene homopolymerization reactions in terms of concentration of TIBA as cocatalyst over different catalysts were studied, the activities and the polymer properties are listed in Table 5. The highest activities of all catalysts were obtained at the Al/Cr molar ratio of 2.5, and among all the catalysts, the activity of (Cr-V-F/3Ti)⁵⁰⁰ was the highest. When the Al/Cr molar ratio increased to 5, the corresponding catalyst activities decreased respectively especially for (Cr-V-F/6Ti)⁵⁰⁰. When the Al/Cr molar ratio increased

Table 4. Comparison of different preparation methods.

	Activation temperature [°C]	Ti [wt%]	Activity [kg _{PE} /mol _{Cr} ·h]	T _m [°C]	MW × 10 ⁵ [g/mol]	MWD
(Cr-V-F) ⁶⁰⁰	600	-	104.0	131.2	5.2	22.7
(Cr-V-F) ⁵⁰⁰	500	-	112.8	131.4	7.3	27.1
(Cr-V-F/3Ti) ⁶⁰⁰	600	3	103.9	131.4	8.9	39.6
(Cr-V-F/3Ti) ⁵⁰⁰	500	3	114.0	131.5	9.2	46.3
(Cr-V-F/6Ti) ⁵⁰⁰	500	6	105.6	131.7	8.7	39.2

Conditions: catalyst 160 mg, ethylene 0.15 MPa, *n*-heptane 70 mL, TIBA as cocatalyst, Al/Cr=2.5, 85 °C, 1 h.

Table 5. Ethylene polymerization of the catalysts and the properties of polymers.

	Al/Cr	Activity [kg _{PE} /mol _{Cr} ·h]	T _m [°C]	Crystallinity [%]	MW × 10 ⁵ [g/mol]	MWD
(Cr-V-F) ⁵⁰⁰	2.5	112.8	131.4	58.6	7.3	27.1
	5	91.5	131.8	62.1	9.5	37.6
	10	57.5	132.4	53.9	9.6	46.9
	15	55.5	132.8	62.5	9.8	46.3
(Cr-V-F/3Ti) ⁶⁰⁰	2.5	103.9	131.4	54.3	8.9	39.6
	5	99.8	132.3	56.9	9.9	40.8
	10	59.2	132.5	62.8	9.4	49.1
	15	54.7	132.4	56.2	10.1	38.4
(Cr-V-F/3Ti) ⁵⁰⁰	2.5	114.0	131.5	64.2	9.2	46.3
	5	95.3	132.4	56.7	11.3	30.7
	10	66.6	132.4	54.8	10.8	51.4
	15	55.0	132.0	52.7	9.1	34.4
(Cr-V-F/6Ti) ⁵⁰⁰	2.5	105.6	131.7	60.2	8.7	39.2
	5	75.6	132.6	57.0	10.5	40.2
	10	57.9	132.5	54.8	13.3	34.7
	15	52.6	132.8	54.2	10.7	47.0

Conditions: catalyst 160 mg, ethylene 0.15 MPa, *n*-heptane 70 mL, TIBA as cocatalyst, 85 °C, 1 h.

to 10 and 15, the corresponding catalyst activities decreased to a similar level of 55 kg_{PE}/mol_{Cr}·h or so. The MW of polyethylene over (Cr-V-F)⁵⁰⁰ rose while the Al/Cr molar ratio increased. But, the MW variation trend of titanium- and fluorine-modified bimetallic catalysts firstly rose up and then dropped down with the increasing Al/Cr molar ratio. It seemed that the addition of TIBA cocatalysts improved the reaction of chain transfer to cocatalysts, giving a higher MW. However, multi-active species on the titanium- and fluorine-modified bimetallic catalysts responded to the TIBA in a divergent way, based on a view of the MW variation trend.

Hydrogen is often used as a chain transfer agent to tailor the polymer MW [47]. The H₂ response of chromium oxide catalyst is not as sensitive as that of Ziegler-Natta or chromocene catalysts [1, 48]. The H₂ sensitivity of chromium oxide catalyst can vary considerably, depending on the support and activation temperature, suggesting that various sites respond quite differently [1]. The addition of H₂ to the reactor usually has no detrimental effect on the activity of chromium oxide catalyst [1]. Hydrogen response reactions over the (Cr-V-F)⁵⁰⁰, (Cr-V-F/3Ti)⁶⁰⁰, and (Cr-V-F/3Ti)⁵⁰⁰ catalysts were performed in the presence of 10 mL H₂ at 85°C and at 0.15 MPa pressure with TIBA as cocatalyst and the Al/Cr molar ratio of 2.5 for the all catalysts. The kinetic curves of the (Cr-V-F)⁵⁰⁰, (Cr-V-F/3Ti)⁶⁰⁰, and (Cr-V-F/3Ti)⁵⁰⁰ catalysts with TIBA as cocatalyst are shown in Figure 2. The ethylene consumptions of polymerization without H₂

over (Cr-V-F/3Ti)⁶⁰⁰ and (Cr-V-F/3Ti)⁵⁰⁰ were more constant and stable than that of (Cr-V-F)⁵⁰⁰. Therefore, the stabilization performance over titanated bimetallic catalyst in polymerization was brought by the addition of titanium. The ethylene consumptions of (Cr-V-F/3Ti)⁶⁰⁰ and (Cr-V-F/3Ti)⁵⁰⁰ were enhanced after the injection of H₂ at the earlier stage of polymerization as depicted in Figure 2. However, at the later stage of polymerization there was a fast decay of polymerization rates, obviously seen in Figure 2. Nonetheless, the performance of (Cr-V-F/3Ti)⁵⁰⁰ depicted in the kinetic curves was more stable than that of the other two and also the activity increased after H₂ addition as summarized in Table 6. One possible explanation for above phenomena is that there are several types of active sites on the bimetallic catalysts and the H₂ not only awakened one type of active sites, namely fast activated and fast decayed active sites, but also killed some active sites which could be activated at the later stage of polymerization. In the study of Phillips catalyst, H₂ affected the active sites unequally too. Ajjou et al. [49] suggested that H₂ caused propagation sites which were less active or even inactive in the absence of H₂ to become more active. These active sites could be protected by the introduction of titanium onto the silica surface, meanwhile a higher activation temperature was unfavorable. A remarkable drop of polymer MW was observed after H₂ added to the reactor, though the extent of reduction in polymer MW of Ti/F-modified bimetallic catalysts was smaller than that of F-modified bimetallic catalysts as listed in

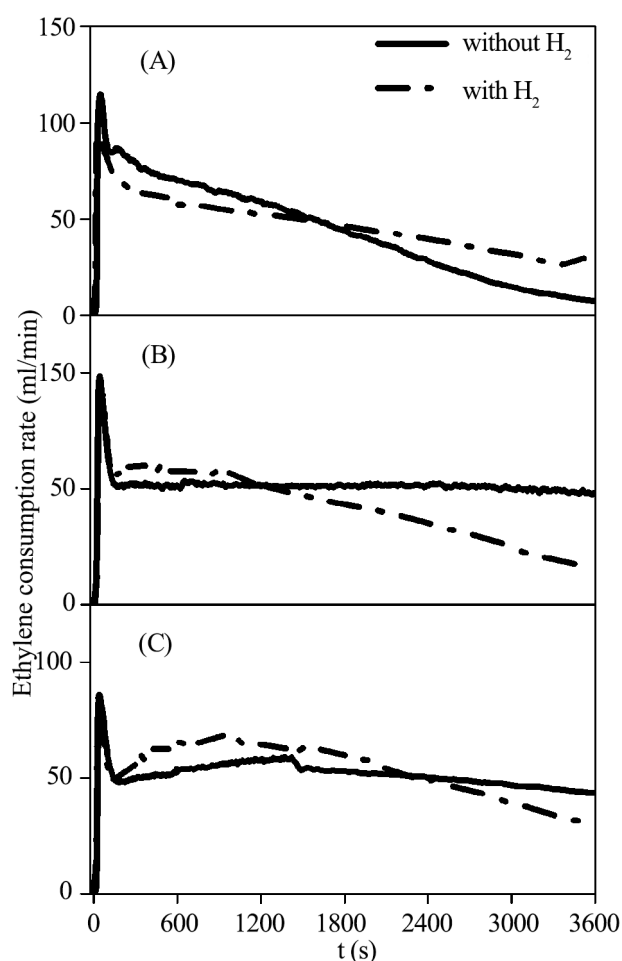


Figure 2. Kinetic curves of ethylene homopolymerization carried out by different catalysts with or without H₂: (A) (Cr-V-F)⁵⁰⁰, (B) (Cr-V-F/3Ti)⁶⁰⁰, and (C) (Cr-V-F/3Ti)⁵⁰⁰.

Table 6. In the presence of H₂, the MW of polymers obtained from the (Cr-V-F/3Ti)⁶⁰⁰ and (Cr-V-F/3Ti)⁵⁰⁰ catalysts decreased by 39.3 % and 32.6 %, respectively, while the MW of the polymer obtained from the (Cr-V-F)⁵⁰⁰ catalyst decreased by 41.1 % as listed in Table 6. Additionally, the MWD of polymers obtained from the (Cr-V-F/3Ti)⁵⁰⁰ and (Cr-V-F/3Ti)⁶⁰⁰ catalyzed H₂ response experiments was narrower than that of polymers obtained from homopolymerization without

H₂, respectively. The lower MW parts increased while the higher MW parts decreased. It was notable that the MWD of (Cr-V-F/3Ti)⁶⁰⁰ and (Cr-V-F/3Ti)⁵⁰⁰ were distorted less than that of (Cr-V-F)⁵⁰⁰ according to the GPC curves presented in Figure 3. In short, the titanium- and fluorine- modified Cr-V bimetallic catalysts had a sensitive hydrogen response.

Copolymerization behavior of different bimetallic catalysts

α -Olefins such as 1-butene, 1-hexene, and 1-octene are used to copolymerize with ethylene in order to add to branches into the main chain of polyethylene as SCB [1, 2, 4, 48, 50]. 1-Hexene is the most commonly used α -olefins due to the better branch insertion and longer branch length [51]. Ethylene/1-hexene copolymerization reactions over bimetallic catalysts were operated in the presence of 1-hexene at 85°C under pressure of 0.15 MPa with TIBA as cocatalyst and the Al/Cr molar ratio of 2.5. The detailed results of the ethylene/1-hexene copolymerization are listed in Table 7 and Figure 4. The activities of (Cr-V-F/3Ti)⁶⁰⁰ were enhanced by adding 0.7 mL and 2.1 mL 1-hexene with a small change in MW and MWD. It might be explained that 1-hexene was helpful to reduce active species at earlier copolymerization stage, although in the literature reports there was still a tremendous dispute on 1-hexene effect over chromium-based catalyst [50, 52]. The activities of (Cr-V-F/3Ti)⁵⁰⁰ decreased with the addition of comonomer and had a fast decay at the later copolymerization stage as opposed to that of (Cr-V-F/3Ti)⁶⁰⁰. These phenomena further illustrated that the active species were highly hybrid on multi-component catalysts and performed diversely under different reaction conditions. The incorporation of 1-hexene was significantly inhibited by the presence of titanium species on (Cr-V-F)⁶⁰⁰ because the incorporated SCB of the copolymers obtained from (Cr-V-F)⁶⁰⁰ was 1.01 mol%, while that

Table 6. Effect of the hydrogen on the activities of catalysts and the properties of polymers.

	H ₂ [mL]	Activity [kg _{PE} /mol _{Cr} ·h]	T _m [°C]	Crystallinity [%]	MW ×10 ⁵ [g/mol]	MWD
(Cr-V-F) ⁵⁰⁰	0	112.8	131.4	58.6	7.3	27.1
	10	100.4	131.6	55.2	4.3	30.1
(Cr-V-F/3Ti) ⁶⁰⁰	0	103.8	131.4	54.3	8.9	39.6
	10	94.1	131.6	66.3	5.4	34.6
(Cr-V-F/3Ti) ⁵⁰⁰	0	113.9	131.5	64.2	9.2	46.3
	10	115.9	131.3	57.0	6.2	38.2

Conditions: catalyst 160 mg, ethylene 0.15 MPa, *n*-heptane 70 mL, TIBA as cocatalyst, Al/Cr=2.5, 1 h.

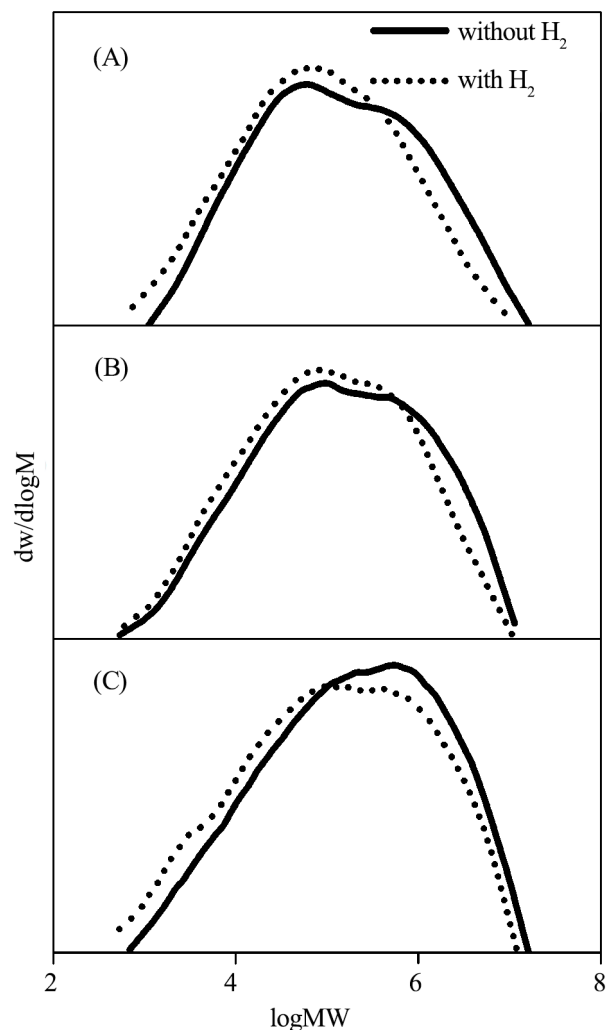


Figure 3. GPC curves of ethylene homopolymerization carried out by different catalysts with (a) 0 mL H₂ and (b) 10 mL H₂: (A) (Cr-V-F)⁶⁰⁰, (B) (Cr-V-F/3Ti)⁶⁰⁰, and (C) (Cr-V-F/3Ti)⁵⁰⁰.

of those obtained from (Cr-V-F/3Ti)⁶⁰⁰ was 0.73 mol% (HT-¹³C NMR spectra were shown in the Supporting

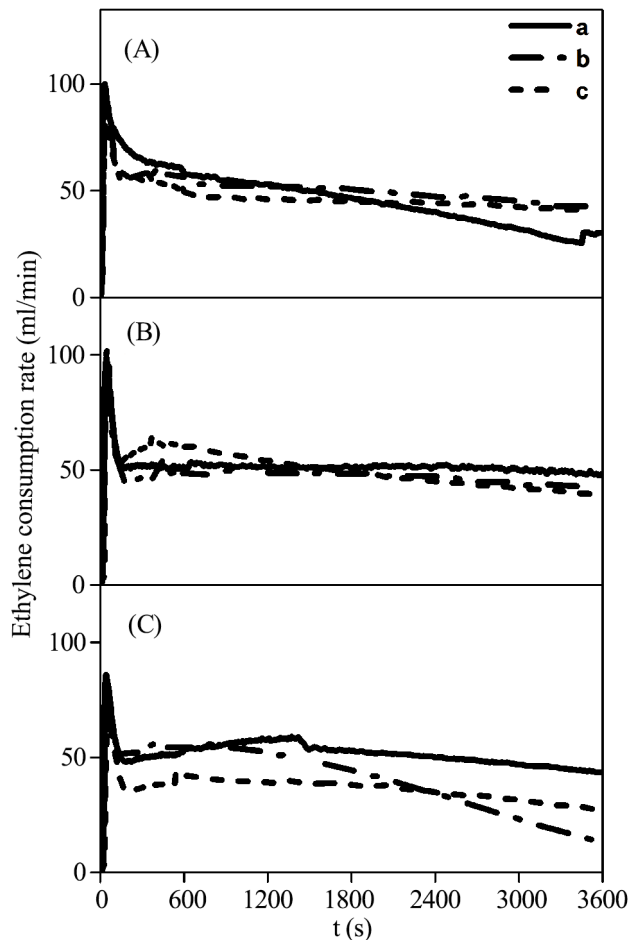


Figure 4. Kinetic curves of ethylene copolymerization carried out by different catalysts with (a) 0 mL, (b) 0.7 mL, and (c) 2.1 mL 1-hexene: (A) (Cr-V-F)⁵⁰⁰, (B) (Cr-V-F/3Ti)⁶⁰⁰, and (C) (Cr-V-F/3Ti)⁵⁰⁰.

Information [Figure S2](#)).

The SCBD for copolymers from different catalysts

The copolymers obtained from (Cr-V-F)⁶⁰⁰ and (Cr-

Table 7. Ethylene/1-hexene copolymerization activities of the catalysts and the properties of polymers.

	1-hexene [ml]	Activity [kg _{PE} /mol _{Cr} ·h]	T _m [°C]	Crystallinity [%]	MW ×10 ⁵ [g/mol]	MWD
(Cr-V-F) ⁶⁰⁰	0	105.0	131.2	61.0	5.2	22.7
	0.7	73.8	131.7	55.6	4.5	20.9
	2.1	61.3	131.5	54.9	3.5	16.9
(Cr-V-F) ⁵⁰⁰	0	112.8	131.4	58.6	7.3	27.1
	0.7	112.3	132.7	52.3	8.3	43.1
	2.1	111.8	131.8	53.1	6.7	46.5
(Cr-V-F/3Ti) ⁶⁰⁰	0	103.8	131.4	54.3	8.9	39.6
	0.7	112.5	132.0	53.1	8.9	41.9
	2.1	121.2	131.5	53.0	8.8	42.4
(Cr-V-F/3Ti) ⁵⁰⁰	0	114.0	131.5	64.2	9.2	46.3
	0.7	88.2	131.2	61.3	9.0	52.4
	2.1	76.7	131.4	57.7	8.4	50.2

Conditions: catalyst 160 mg, ethylene 0.15 MPa, *n*-heptane 70 mL, TIBA as cocatalyst, Al/Cr=2.5, 1 h.

Table 8. MW and MWD of the fractions measured by GPC.

Temperature [°C]	PE- 1		PE- 2	
	MW ^(a) ×10 ⁵ [g/mol]	MWD ^(a)	MW ^(a) ×10 ⁵ [g/mol]	MWD ^(a)
≤40	...(b)	...(b)	0.010	2.0
40-60	0.035	4.5	0.019	1.7
60-70	0.24	10.0	0.024	1.6
94-95	6.9	14.3	0.26	1.8
103-108	5.7	2.8	11.3	3.3
108-115	6.2	3.7	10.0	2.8
115-124	4.7	2.9	8.8	2.4

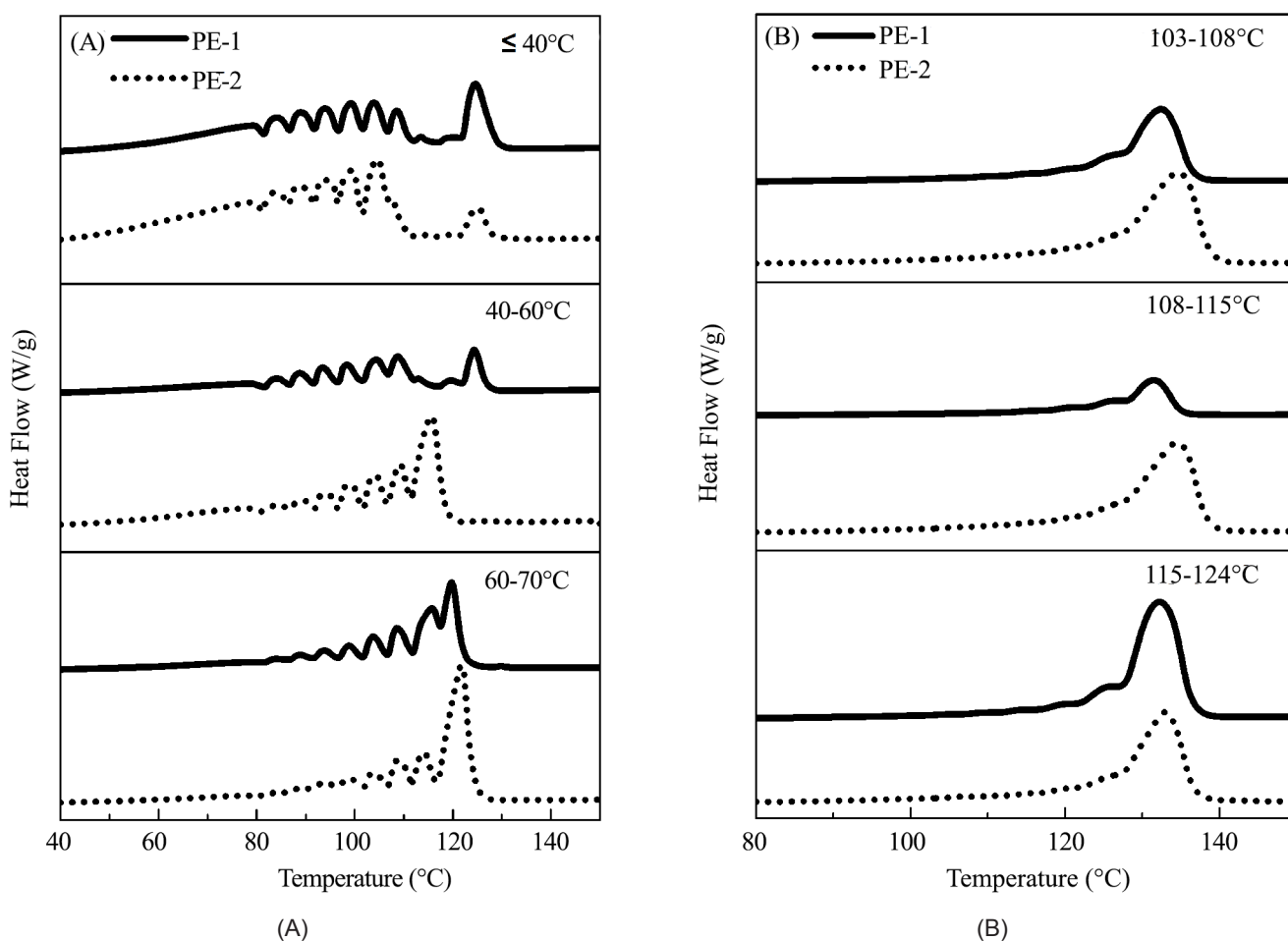
(a) MW was estimated by GPC in TCB vs PS stds, MWD (M_w/M_n).

(b) Too little to characterize.

V-F/3Ti)⁶⁰⁰ donated, respectively, as PE-1 and PE-2 were investigated by both TREF and SSA. The two weight distributions of fractions obtained at a certain crystalline temperature of the two copolymers samples were narrow as a typical HDPE with few low-temperature and high-temperature fractions as shown in Figure S3. The temperature intervals of maximum weight fraction from PE-1 and PE-2 were all 94-95°C.

The overall trends of MW results corresponding to temperature fractions listed in Table 8 conformed to the conclusion that the low-temperature fractions corresponded to the low average MW part, while the high-temperature fractions corresponded to the high average MW part [18]. The MW of low-temperature fractions from PE-2 is lower than that from PE-1, while the MW of high-temperature fractions from PE-2 is higher than that from PE-1.

SSA characterization was applied to analyze and characterize the SCBD of low- and high-temperature fractions of PE-1 and PE-2. The results are illustrated in Figure 5. The numbers and intensities of the melting peaks in the DSC-SSA curves can be used to evaluate the intra-molecular composition distribution qualitatively. The melting peak intensities of PE-1 in higher-melting temperature were stronger than those of PE-2 as depicted in Figure 5 (A). It was suggested that there was less 1-hexene insertion into the fractions of PE-1. The melting peaks in high-temperature fractions of PE-2 rose at the slightly higher-melting temperature

**Figure 5.** DSA-SSA curves of the fractions for copolymers, (A) low-temperature fractions and (B) high-temperature fractions.

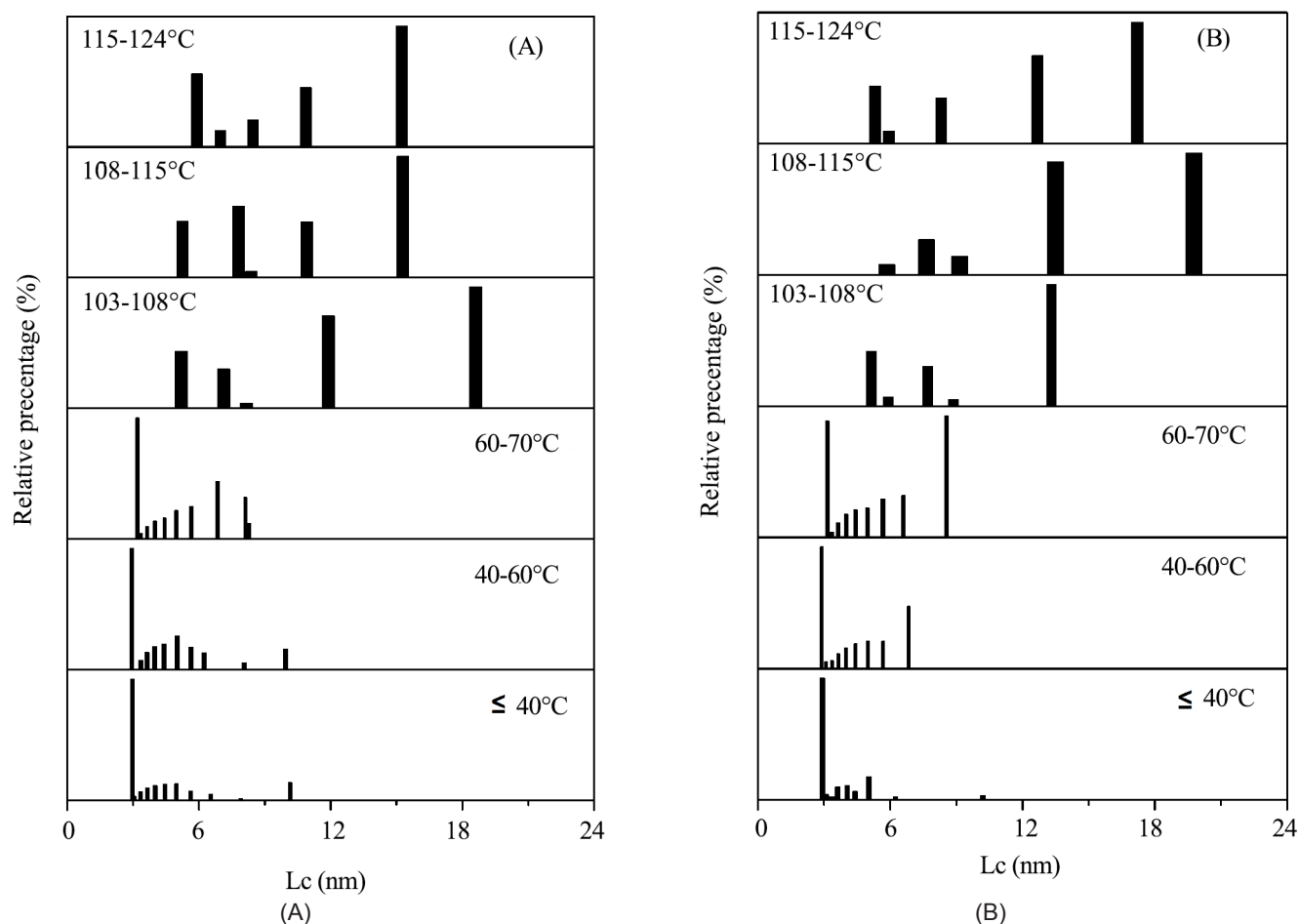


Figure 6. Distribution of lamella thickness of certain fractions of copolymers, (A) PE-1 and (B) PE-2.

and had higher peak intensities in 103-108°C and 108-115°C fractions than those of PE-1 as depicted in Figure 5 (B), suggesting a slightly lower degree of comonomer insertion into the higher MW fractions of PE-2. The modified Thomas Gibbs equation (as shown in Equation 1) was used to set up a correlation between melting point and lamella thickness for the comparison of the SCBD of the two copolymer samples. The lamella thickness was greatly affected by the content of SCB in each fraction of copolymer samples and the more comonomer insertion resulted in the thinner lamella thickness, where the melting point of linear polyethylene was close to 145°C. The lamella thickness was calculated using the melting point value of each endothermal peak relating to a copolymer fraction in the SSA curves after peak fitting, lamellar surface free energy σ (5.0 kJ/mol), enthalpy of fusion of per C_2H_4 group (8.2 kJ/mol), and length of C_2H_4 unit in chain direction (0.254 nm) [29, 53].

$$L = \frac{2\sigma T_{mp}^{\circ} \Delta z}{\Delta h(T_{mp}^{\circ} - T_{mp})} \quad (1)$$

The lamella thickness distributions of certain fractions of PE-1 and PE-2 are illustrated in Figure 6. Through the comparison of the lamella thickness distribution of the two copolymers in the higher temperature fractions (corresponding to the higher MW part), it was illustrated that the lamella thickness of PE-1 was thinner than that of PE-2. This result indicated that the corresponding relative SCB content of copolymers in the higher MW part obtained from $(Cr-V-F)^{600}$ was higher than that obtained from the $(Cr-V-F/3Ti)^{600}$ catalyst. In the lower temperature fractions (corresponding to the lower MW part), the copolymers PE-2 obtained from $(Cr-V-F/3Ti)^{600}$ showed much thinner lamella thickness (corresponding much higher relative SCB content) than PE-1. The results were consistent with the corresponding DSC- SSA curves presented in Figure 5 (A), in which the PE-2 had less apparent higher-temperature melting peaks in the DSC-SSA curves. Considering the MW results listed in Table 8, there was more relative SCB content in

lower MW part but less relative SCB content in higher MW part of PE-2 than that of PE-1. Therefore, the results showed that the introduction of titanium species increased the SCB content in low MW fractions and decreased the SCB content in the high Mw fractions of ethylene/1-hexene copolymers obtained from (Cr-V-F/3Ti)⁶⁰⁰ in contrast to (Cr-V-F)⁶⁰⁰.

CONCLUSION

In this work, titanium- and fluorine- modified chromium-vanadium bimetallic catalysts (Cr-V-F/Ti) were prepared by incorporation of titanium species onto the silica surface as the catalyst supports. The ethylene homopolymerization experiments, H₂ response experiments, and copolymerization behaviors of catalysts with 1- hexene were systematically investigated and compared with those for the fluorine-modified Cr-V bimetallic (Cr-V-F) catalysts. Nitrogen adsorption/desorption experiments showed that the surface area, pore volume, and average pore size of all catalysts remained well. The introduction of titanium into the Cr-V-F catalysts enhanced the MW and broadened the MWD of polyethylene. The MW variation trend of the novel modified Cr-V bimetallic catalysts firstly rose up and then dropped with the increasing of the Al/Cr molar ratio. The Cr-V-F/Ti catalysts showed slightly depressed hydrogen response and incorporation of 1-hexene. To reiterate, the active species were highly hybridized with multi-component catalysts and performed diversely under different reaction conditions. The results of TREF/SSA showed that the Ti-modification increased the SCB content in low MW fractions and decreased the SCB content in the high MW fractions of ethylene/1-hexene copolymers obtained from (Cr-V-F/3Ti)⁶⁰⁰ in contrast to that from (Cr-V-F)⁶⁰⁰.

ACKNOWLEDGEMENTS

We gratefully thank the financial support by the National Natural Science Foundation of China (No. 21104019 and 21274040), and the Major State Basic Research Development Program of China (2012CB720502). This work is also financially supported by the Fundamental Research Funds for the

Central Universities, research program of Introducing Talents of Discipline of university (B08021), and research program of the State Key Laboratory of Chemical Engineering.

REFERENCES

1. McDaniel MP (2010) A review of the Phillips supported chromium catalyst and its commercial use for ethylene polymerization. In: Handbook of transition metal polymerization catalysts, John Wiley & Sons, 123-606
2. McDaniel MP (2008) Review of the Phillips chromium catalyst for ethylene polymerization. In: Handbook of heterogeneous catalysis, Wiley-VCH, 3733-3792
3. Liu Z, He X, Cheng R, Eisen MS, Terano M, Liu B (2013) Chromium catalysts for ethylene polymerization and oligomerization. In: Advances in Chemical Engineering, Elsevier, 127-191
4. McDaniel MP (1985) Supported chromium catalysts for ethylene polymerization. *Adv Catal* 33: 47-98
5. Cheng R, Liu Z, Zhong L, He X, Qiu P, Terano M, Eisen MS, Scott SL, Liu B (2013) Phillips Cr/silica catalyst for ethylene polymerization. In: Polyolefins: 50 years after Ziegler and Natta I, Springer, 135-202
6. Clark A, Hogan JP, Banks RL, Lanning WC (1956) Marlex catalyst systems. *Ind Eng Chem* 48: 1152-1155
7. McDaniel MP (1983 Sep. 20) Polymerization process using chromium on a support treated with titanium polymer, US Patent 4,405,768
8. Rebenstorf B, Sheng TC (1991) Influence of chromium concentration and addition of fluorine, titanium, or boron on the chromium species of the Phillips catalyst: A quantitative evaluation. *Langmuir* 7: 2160-2165
9. Hawley GR (1981 Oct. 20) Titanium impregnated silica-chromium catalysts, US Patent 4,296,001
10. Dreiling MJ (1983) The activation of the Phillips polymerization catalyst III. Promotion by titania. *J Catal* 82: 118-126

11. Cheng R, Xu C, Liu Z, Dong Q, He X, Fang Y, Terano M, Hu Y, Pullukat TJ, Liu B (2010) High-resolution spectroscopy (XPS, ^1H mas solid-state NMR) and DFT investigations into Ti-modified Phillips $\text{CrO}_x/\text{SiO}_2$ catalysts. *J Catal* 273: 103-115
12. Zhong L, Liu Z, Cheng R, He X, Liu B (2013) Effect of fluorination of silica support on initiation of ethylene polymerization during induction period over Phillips catalyst. *J Chem Ind Eng (China)* 64: 539-546
13. Hogan JP (1964 Apr. 21) Catalyst and process for producing olefin polymers, US Patent 3,130,188
14. Nasser Jr. BED, Richard E. (1978 Dec. 19) Two stage activation of fluorided chromium-containing catalyst, US Patent 4,130,505
15. McDaniel MP (1985 Oct. 15) Silica-titania cogel from two-step hydrolysis, US Patent 4,547,557
16. Dwivedi S, Gujral SS, Taniike T, Terano M (2013) Chemical modification of silica support to improve the branching ability of Phillips catalyst. *Pure Appl Chem* 85: 533-541
17. McDaniel MP, Johnson MM (1986) A comparison of chromium/silica and chromium/aluminum phosphate polymerization catalysts. I. Kinetics. *J Catal* 101: 446-457
18. Zhang S, Dong Q, Cheng R, He X, Wang Q, Tang Y, Yu Y, Xie K, Da J, Liu B (2012) A novel SiO_2 - supported inorganic and organic hybrid chromium-based catalyst for ethylene polymerization. *J Mol Catal A: Chem* 358: 10-22
19. Zhang S, Cheng R, Dong Q, He X, Wang Q, Tang Y, Yu Y, Xie K, Da J, Terano M (2013) Ethylene/1-hexene copolymerization with a novel SiO_2 -supported inorganic and organic hybrid chromium-based catalyst. *Macromol React Eng* 7: 254-266
20. Cheng R, Xue X, Liu W, Zhao N, He X, Liu Z, Liu B (2015) Novel SiO_2 -supported chromium oxide(Cr)/vanadium oxide(V) bimetallic catalysts for production of bimodal polyethylene. *Macromol React Eng* 9: 462-472
21. Matta A, Zeng Y, Taniike T, Terano M (2012) Vanadium-modified bimetallic Phillips catalyst with high branching ability for ethylene polymerization. *Macromol React Eng* 6: 346-350
22. Zeng Y, Matta A, Dwivedi S, Taniike T, Terano M (2013) Development of a hetero-bimetallic Phillips-type catalyst for ethylene polymerization. *Macromol React Eng* 7: 668-673
23. McDaniel MP (1982) The state of Cr(VI) on the Phillips polymerization catalyst. IV. Saturation coverage. *J Catal* 76: 37-47
24. Bernd R (1991) The Phillips catalyst (Cr(VI)/silica gel) modified by $(\text{NH}_4)_2\text{SiF}_6$: Its influence on the chromium surface species. *J Mol Catal* 66: 59-71
25. Levine IJ, Karol FJ (1976 Mar. 8) Preparation of low and medium density ethylene polymer in fluid reactor, US Patent 4,011,382
26. Seger MR, Maciel GE, Chem. A (2004) Quantitative ^{13}C NMR analysis of sequence distributions in poly(ethylene-co-1-hexene). *Anal Chem* 76: 5734-5747
27. Ma Y, Cheng R, Li J, Zhong L, Liu Z, He X, Liu B (2015) Effect of Mo-modification over Phillips $\text{CrO}_x/\text{SiO}_2$ catalyst for ethylene polymerization. *J Organomet Chem* 791: 311-321
28. Zhao N, Cheng R, He X, Liu Z, Liu B (2014) A novel SiO_2 -supported Cr-V bimetallic catalyst making polyethylene and ethylene/1-hexene copolymers with bimodal molecular weight distribution. *Macromol Chem Phys* 215: 1753-1766
29. Müller AJ, Arnal ML (2005) Thermal fractionation of polymers. *Prog Polym Sci* 30: 559-603
30. Tanem BS, Stori A (2001) Phase separation in melt blends of single-site linear and branched polyethylene. *Polymer* 42: 5689-5694
31. Müller AJ, Hernández ZH, Arnal ML, Sánchez JJ (1997) Successive self-nucleation/annealing (SSA): A novel technique to study molecular segregation during crystallization. *Polym Bull* 39: 465-472
32. Pullukat TJ, Hoff RE, Shida M (1980) A chemical study of thermally activated chromic titanate on silica ethylene polymerization catalysts. *J Polym Sci A Polym Chem* 18: 2857-2866
33. Hoff RE, Pullukat TJ, Shida M (1981) Chromic titanate catalysts for high-melt-index

- polyethylene by the particle-form process. *J Appl Polym Sci* 26: 2927-2934
34. Gao X, Wachs IE (2002) Molecular engineering of supported vanadium oxide catalysts through support modification. *Top Catal* 18: 243-250
 35. Gao X, Bare SR, Fierro J, Wachs IE (1999) Structural characteristics and reactivity/reducibility properties of dispersed and bilayered V₂O₅/TiO₂/SiO₂ catalysts. *J Phys Chem B* 103: 618-629
 36. Mohamadnia Z, Ahmadi E, Nekoomanesh M, Ramazani A, Mobarakeh HS (2010) Effect of support structure on the activity of Cr/nanosilica catalysts and the morphology of prepared polyethylene. *Polym Int* 59: 945-953
 37. Ahmadi E, Mohamadnia Z, Rahimi S, Armanmehr MH, Razmjoo M, Heydari MH (2016) Phillips catalysts synthesized over various silica supports: Characterization and their catalytic evaluation in ethylene polymerization. *Polyolefins J* 3: 23-36
 38. McDaniel MP, Collins KS (2009) The influence of porosity on the Phillips Cr/silica catalyst 2. Polyethylene elasticity. *J Polym Sci, Part A: Polym Chem* 47: 845-865
 39. Marsden CE (1991) The influence of silica support on polymerisation catalyst performance. In: *Preparation of catalysts V: Scientific bases for the preparation of heterogeneous catalysts*, proceedings of the fifth international symposium, Elsevier, 215-227
 40. Liu B, Sindelar P, Fang Y, Hasebe K, Terano M (2005) Correlation of oxidation states of surface chromium species with ethylene polymerization activity for Phillips CrO_x/SiO₂ catalysts modified by Al-alkyl cocatalyst. *J Mol Catal A-Chem* 238: 142-150
 41. Xia W, Liu B, Fang Y, Hasebe K, Terano M (2006) Unique polymerization kinetics obtained from simultaneous interaction of Phillips Cr(VI) O_x/SiO₂ catalyst with Al-alkyl cocatalyst and ethylene monomer. *J Mol Catal A-Chem* 256: 301-308
 42. Xia W, Tonosaki K, Taniike T, Terano M, Fujitani T, Liu B (2009) Copolymerization of ethylene and cyclopentene with the Phillips CrO_x/SiO₂ catalyst in the presence of an aluminum alkyl cocatalyst. *J Appl Polym Sci* 111: 1869-1877
 43. Xia W, Liu B, Fang Y, Fujitani T, Taniike T, Terano M (2010) Multinuclear solid-state NMR study of the coordinative nature of alkylaluminum cocatalyst on Phillips CrO_x/SiO₂ catalyst. *Appl Catal, A-Gen* 389: 186-194
 44. Krauss HL, Hanke B (1985) Surface compounds of transition metals. XXIX. Reaction of surface chromium(VI)/silica gel with aluminium alkyls: "Formation" of Phillips catalysts. *Z Anorg Allg Chem* 521: 111-121
 45. Krauss HL (1988) New results with Phillips systems: Surface compounds of transition metals, Part XXXII. *J Mol Catal* 46: 97-108
 46. Iwasawa Y, Sasaki Y, Ogasawara S (1982) Active fixed chromium catalysis for co-oxidation. Preparation and active structure of fixed Cr and Cr₂ catalysts. *J Mol Catal* 16: 27-41
 47. Hogan JP (1970) Ethylene polymerization catalysis over chromium oxide. *J Polym Sci, Part Pol Chem* 8: 2637-2652
 48. Soares JBP, Mckenna TFL (2013) *Polyolefin Reaction Engineering*. Weinheim, Germany, Wiley-VCH
 49. Ajjou JaN, Scott SL (2000) A kinetic study of ethylene and 1-hexene homo- and copolymerization catalyzed by a silica-supported Cr(IV) complex: Evidence for propagation by a migratory insertion mechanism. *J Am Chem Soc* 122: 8968-8976
 50. McDaniel MP, Schwerdtfeger ED, Jensen MD (2014) The "comonomer effect" on chromium polymerization catalysts. *J Catal* 314: 109-116
 51. Clark A (1970) Olefin polymerization on supported chromium oxide catalysts. *Cat Rev* 3: 145-173
 52. Rangwala HA, Dalla Lana IG, Szymura JA, Fiedorow RM (1996) Copolymerization of ethylene and 1-butene using a Cr-silica catalyst in a slurry reactor. *J Polym Sci Pol Chem* 34: 3379-3387
 53. Lorenzo AT, Arnal ML, Müller AJ, Fierro ABD, Abetz V (2006) High speed SSA thermal fractionation and limitations to the determination of lamellar sizes and their distributions. *Macromol Chem Phys* 207: 39-49